

Chapter 1

Fundamentals of Cold Spray Processing: Evolution and Future Perspectives

Bandar AlMangour

1.1 Introduction

1.1.1 Motivations and Outline of the Chapter

Metal coatings can be deposited by multiple thermal spraying techniques, such as high-velocity oxygen fuel (HVOF) and plasma spraying. In these spraying processes, the feedstock powders can melt significantly (Sampath et al. 2004). This can generate coatings with high residual stresses, crack formation, material oxidation, and phase transformation, all of which can influence the physical, electrochemical, and mechanical properties of the coatings (Sampath et al. 2004). A recently introduced spraying technique called cold-gas dynamic spraying, or simply cold spraying (CS), was initially developed at the Institute of Theoretical and Applied Mechanics in Russia (Dykhuzen and Smith 1998; Irissou et al. 2007). In this process, particles with micrometer-scale sizes are accelerated by a relatively low-temperature gas jet to a high velocity, accumulating into dense coatings on impact (Grujicic et al. 2004a; Van Steenkiste and Smith 2004; Marx et al. 2006).

In contrast to thermal spraying technologies, powder melting is infrequent in CS, because kinetic energy provides the major driving force for powder consolidation and adhesion to the substrate via metallurgical bonding (Gärtner et al. 2006a). The relatively low processing temperatures increase the possibility of retaining the microstructures and properties of the feedstock materials (Irissou et al. 2008). CS belongs to the family of thermal spray methods but differs from other techniques in being a solid-state process, wherein the sprayed particles are deposited through

B. AlMangour (✉)
School of Engineering and Applied Sciences, Harvard University,
Cambridge, MA 02138, USA
e-mail: balmangour@seas.harvard.edu; balmangour@gmail.com

supersonic velocity impact with the substrate at temperatures far below the melting point of the sprayed material. Adhesion occurring in the solid state lends distinctive features to CS deposits and makes CS appropriate for depositing both traditional and advanced materials on several substrate material types, including in temperature-sensitive applications (Champagne 2007).

Successful bonding in CS is associated with the degree of particle deformation during impact and increases in temperature at the particle–particle and particle–substrate interfaces (Assadi et al. 2003). In other words, increased plastic flow by adiabatic shear instability is necessary for bonding (Assadi et al. 2003; Schmidt et al. 2006). The adhesion of the powder to the substrate depends on whether it exceeds a critical velocity, which varies among powders (Gilmore et al. 1999). The critical velocity in CS is generally a function of material properties (Stoltenhoff et al. 2002).

Since its discovery, CS has undergone much development; current CS technology is utilized in an expanding range of industries for many applications, mainly in surface restoration, as well as the wear-resistant and corrosion-resistant repair of metals and alloys. Several international organizations continue to develop the CS technology to fulfill the needs of high-performance applications. This chapter outlines current knowledge in CS by reviewing the fundamentals of the CS process and its features, applications, and bonding mechanisms in brief, and also provides an overview of recent and emerging developments in the process and the future potential of this technology. The different aspects of CS are addressed in the context of the essential parameters affecting deposition behavior. The merits, limitations, and applications of the process are also described.

1.1.2 Historical Background

The cold gas dynamic spray process was initially invented and patented by Dr. Anatolii Papyrin and his colleagues at the Institute of Theoretical and Applied Mechanics at Novosibirsk, Russia, in the mid-1980s (Alkhimov et al. 1990). The researchers were conducting experiments in a wind tunnel subjected to a supersonic two-phase flow of gas and solid metallic particles, studying the effects of the particles on the flow structure and the interaction of the two-phase flow with a body (Alkhimov et al. 1990). They observed that, under specific conditions, fine particles injected in the flow stream were deposited on the leading edges of the model bodies. As the particle velocity was increased, the effect of impact transformed from the erosion of the substrate to the rapid accumulation of a coating (Alkhimov et al. 1990; Champagne 2007). The scientists realized the potential of this phenomenon as a new alternative coating procedure and developed a spray coating machine based on the principle. They successfully deposited many different metals, alloys, and composites onto multiple substrate materials, demonstrating the suitability of CS for numerous uses (Alkhimov et al. 1990; Champagne 2007).

1.2 General Process Overview

The CS process is an advanced coating technique in which solid powder particles (1–100 μm in diameter) are accelerated to speeds reaching 1500 m/s by a supersonic gas jet. The powder particles undergo significant deformation on impact with the substrate, thereby forming a coating. The quality of the coating depends on the powder and substrate types, as well as the processing parameters, such as the gas pressure and type, gas temperature, standoff distance, and particle velocity (Champagne 2007).

As shown in Fig. 1.1, CS appears very simple. First, a high-pressure gas supply of nitrogen, helium, or a mixture of these is compressed to 1.0–4.0 MPa and flowed through the system in two different paths. The first path passes through the powder feeder in order to transport the particles to the gun. A typical CS gun is equipped with a converging/diverging de Laval-type nozzle, which permits the gas and particles to reach supersonic velocities (Papyrin et al. 2006; Maev and Leshchynsky 2008). The second path travels through an electric gas heater and is preheated to temperatures of 100–800 $^{\circ}\text{C}$ (Maev and Leshchynsky 2008). This provides an additional increase to the gas velocity and, consequently, increases the particle velocity. The two paths converge near the nozzle entrance (Maev and Leshchynsky 2008). Finally, the feedstock powders reach supersonic velocities, exit the gun nozzle, and collide with the substrate to form a coating (Maev and Leshchynsky 2008). Although the inlet gas is preheated to high temperatures, the particles remain solid in state because the time of contact between the high-temperature gas and particles is relatively short; the gas temperature is also often much lower than the melting point of the powder. In addition, the temperature of the gas is decreased significantly with the expansion of the divergent section of the gun nozzle (Papyrin et al. 2006).

Although the principle of CS is simple, controlling the process is very difficult owing to the many processing parameters. The type of gas, gas pressure and temperature, powder shape and size, nozzle design, standoff distance, traverse speed, and velocity of the particles all strongly affect the properties of the coating.

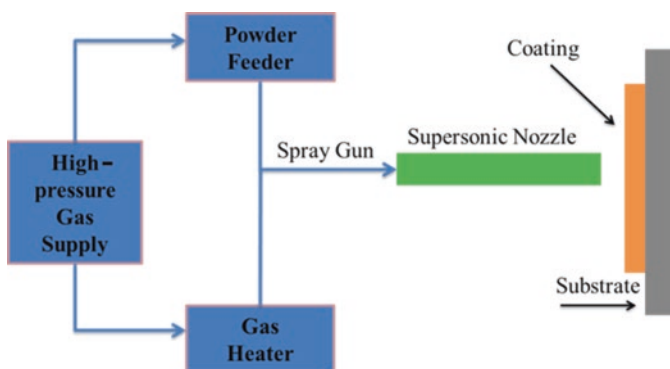


Fig. 1.1 Schematic of the CS process

1.3 Advantages and Limitations of CS

As illustrated in Fig. 1.2, the main differences between CS and other thermal spray processes are the gas temperature and particle velocity. CS utilizes high particle velocities instead of high gas temperatures to form coatings, which has many advantages. CS is suitable for forming coatings of temperature-sensitive materials (Champagne 2007; Irissou et al. 2008), as well as oxygen-sensitive materials such as aluminum, copper, and titanium. In addition, because the feedstock powder is neither heated nor melted in the process, it can be reused in future coating cycles (Champagne 2007). CS is very well suited for restoring damaged metal parts and apparatus in industrial paraphernalia. The addition of coatings to parts comprising the original material of manufacture is an efficient means of improving the equipment performance, without the expense of producing a new part (i.e., cost saving selection) or increasing environmental waste.

Conventional thermal spray processes often entail grain growth, chemical reactions, cracks, evaporation, thermal residual stresses, thermal shrinkage, phase transformation, and oxidation; these are absent in CS (Papyrin et al. 2006). Because CS uses relatively low gas temperatures, it is operationally safer regarding thermal radiation and metal vapors (Champagne 2007). Another advantage is the ability to coat substrates of <1 mm in thickness without substrate damage. Furthermore, the process can produce well-bonded thick coatings or multilayer coatings, because coatings are produced with compressive stresses (Champagne 2007). With high kinetic energy and low gas temperatures, CS can provide coatings with wrought microstructures and low porosities (Champagne 2007). Moreover, because the spray trace is relatively small (1–25 mm²), CS allows the high-efficiency deposition of precise coatings (Ghelichi and Guagliano 2009), although the deposition efficiency does vary with the types of powder being sprayed.

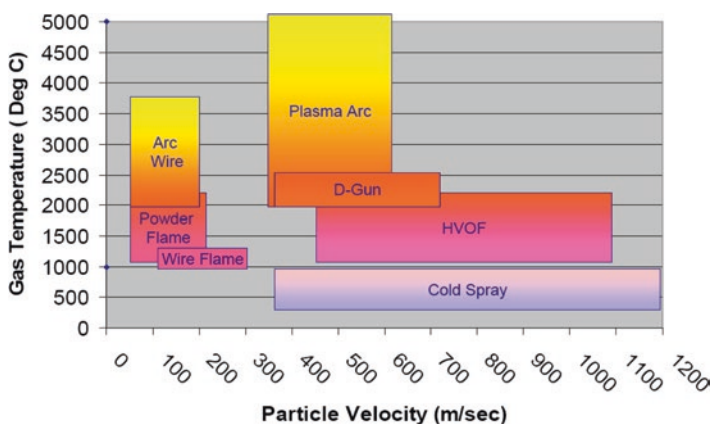


Fig. 1.2 Comparison of CS and thermal spray processing parameters (Champagne 2007)—*D-Gun* detonation gun spraying, *HVOF* high-velocity oxygen fuel

CS, however, does have limitations. One disadvantage that may occur while spraying is nozzle blockage, especially during longer spraying processes; this causes different deposition rates over time and affects the coating properties (Irissou et al. 2008). While CS can utilize a wide range of dissimilar feedstocks and substrates, it is limited to relatively ductile metal powders or hard metals mixed with ductile metals; the technique cannot deposit hard single-species particles such as ceramics (Grujicic et al. 2003). This is because the particles must undergo plastic deformation for interparticle bonding to occur. Similarly, spraying onto ceramic substrates is difficult, with low coating–substrate interfacial bond strength. Furthermore, processing gas consumption is high relative to that in thermal spray processes, typically on the order of 1–2 m³/min (Gärtner et al. 2006a). Indeed, when helium gas is required to maximize the particle velocity, the high cost of this nonrenewable resource becomes a concern.

The smallness of the spray trace, while allowing precise coverage, combined with the short standoff distance causes difficulties in coating large-surface-area substrates. In addition, CS creates as-sprayed coatings with very poor ductility because the structure is very hard and interparticle bonds can be relatively weak (Borchers et al. 2005; Sundararajan et al. 2009). Finally, the quality and microstructure of the powder must be considered. Because the process is relatively low temperature, the compositional aspects of the as-sprayed coatings are equivalent to those of the feedstock, but the microstructure becomes work hardened and recrystallization may occur at particle–particle interfaces (Kim et al. 2005a; Zou et al. 2009). The chemical composition of the feedstock is retained, including its impurities, which then appear in the coating. Accordingly, the powder production stage should be optimized before attempting to produce coatings.

1.4 Applications of CS

Numerous studies have claimed that CS provides coatings with superior corrosion, wear resistance, and mechanical integrity in the as-sprayed condition (Yandouzi et al. 2007). These coatings can be used in many sectors, including the aerospace, automotive, transportation, die casting, petrochemical, mineral and metal processing, electronics, marine, and ceramics and glass manufacturing industries (Marx et al. 2006; Champagne 2007). Table 1.1 shows the potential applications of CS in different industrial sectors.

1.5 Bonding Mechanisms and Powder Consolidation in CS

1.5.1 Bonding Mechanisms

Although many numerical simulations and experimental investigations have been performed to understand the bonding mechanism in CS, it remains poorly understood (Maev and Leshchynsky 2008). Currently, the most likely bonding mechanism

Table 1.1 CS coating materials and applications in different industrial sectors

Application	Coating materials	Industry sector
Corrosion resistance	Al and Ni alloys, Ti, Ta	Aerospace Oil and gas Petrochemical Power generation
Pb-free bearings	Al, Cu alloys	Automotive Motorsport Aerospace
Wear-resistant coatings	WC–Co	Oil and gas
Bio-inert devices	Ti	Medical

in CS is associated with adiabatic shear instability (ASI), as proposed by Assadi et al. (2003). In this mechanism, the particle–particle or particle–substrate interfacial areas experience severe localized shear deformation during impact, which disrupts the thin oxide surface films on the particles, permitting strong particle–substrate contact (Assadi et al. 2003; Schmidt et al. 2006). This phenomenon, combined with the high compressive stresses developed on collision of the particles with the substrate, is necessary for bonding (Assadi et al. 2003; Grujicic et al. 2004a; Schmidt et al. 2006). In other words, the material loses shear strength and undergoes severe deformation such that the deformation mechanism changes from plastic to viscous flow (Assadi et al. 2003; Grujicic et al. 2003). This facilitates the formation of metallurgical bonds (i.e., atomic bonds) of the particles to the substrate, as well as between particles. However, all of the analyses supporting this proposal are based on numerical simulations (Assadi et al. 2003; Grujicic et al. 2003, 2004a), which sometimes deviate from experimental tests.

Bae et al. (2008) have suggested the existence of a thermal boost-up zone (TBZ), which indicates a specific transitional temperature point (i.e., a sharp increase in temperature) before the start of ASI. TBZs are caused by unstable plastic deformation when the rate of thermal softening exceeds the rate of work hardening (Bae et al. 2008). However, in another study performed by the same authors (Bae et al. 2009), in which a simulation of a titanium particle colliding with a titanium substrate was performed, it was shown that the TBZ was not required for successful bonding. Therefore, although ASI is a likely bonding mechanism for CS, successful particle–particle or particle–substrate bonding does not necessarily require the existence of ASI.

Hussain et al. (2009) proposed another bonding mechanism known as mechanical interlocking after cold spraying copper particles onto aluminum substrates. They suggested that the impaction of the copper particles on the aluminum substrate caused lips to form in the aluminum substrate, which partially enveloped the copper particles (Hussain et al. 2009). This created a mechanical interlock between the substrate and impacting particles, as shown in Fig. 1.3.

The powder can adhere to the substrate during CS with high bond strength. Van Steenkiste et al. (2002) suggested that the formation of the coating occurs in four main stages, as demonstrated in Fig. 1.4. First, the substrate is cratered and the first

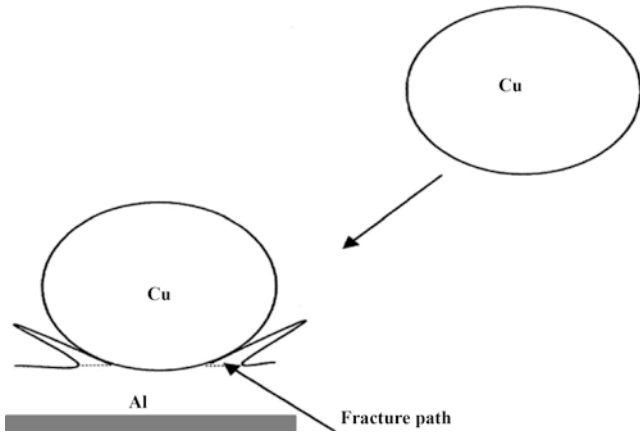


Fig. 1.3 Schematic of jet formation on an aluminum substrate by an approaching Cu particle. The jet is trapped in the copper coating by the incoming copper particles. During bond strength testing, fracture occurs in the aluminum jet, indicated by the *dotted line*. Here, copper and aluminum are examples for the sake of illustration; other metallic species show the same behaviors (Hussain et al. 2009)

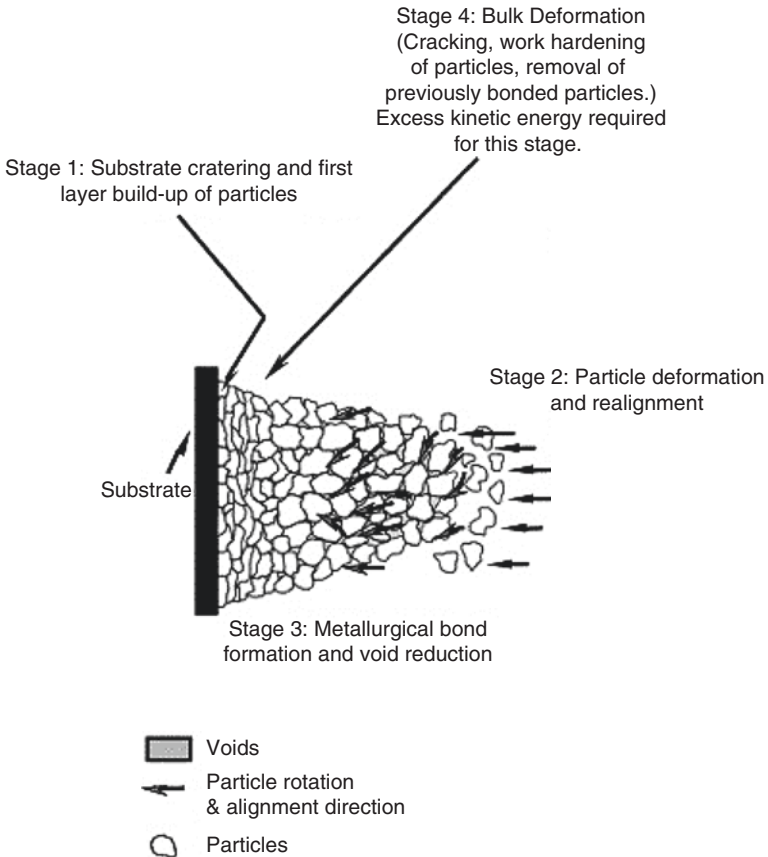


Fig. 1.4 Stages of coating formation in CS (Van Steenkiste et al. 2002)

monolayer of particles is formed. The challenge in this stage relies on particle and substrate conditions, such as roughness, hardness, and temperature (Ghelichi and Guagliano 2009). Next, the approaching particles are deformed, rotated, and readjusted. Then, particle–particle metallurgical bonds form in increasing numbers, creating a thick and hard coating. Finally, as the coating continues to accumulate, the constant shot peening (compressive stress) causes further plastic deformation and work hardening. At a given impact velocity, some of these stages may occur simultaneously (Van Steenkiste et al. 2002).

1.5.2 Cold Sprayability of Materials

The ease with which a metal can be processed by CS, i.e., the cold sprayability, depends largely on the plastic deformation mechanisms of the metal. The deformation mechanisms are usually determined by dislocation motion and interactions, which are dictated mainly by the crystal structure (Amodeo and Ghoniem 1990). Therefore, feedstock powders can be classified according to crystal structure, since similar structures have similar mechanical properties. The most popular group is face-centered cubic (FCC) metals, such as aluminum, copper, nickel, and 316L stainless steel. Metals like tungsten, tantalum, molybdenum, and chromium are body-centered cubic (BCC). Zinc, cobalt, and titanium are hexagonally close packed (HCP). In general, metals with the FCC lattice have the highest number of slip systems, which provide them with the greatest deformability (Borchers et al. 2004; Vlcek et al. 2005). Because metals with HCP and BCC structures have fewer slip systems, they tend to have lower plasticity, making them less suitable for CS processing. More extreme processing parameters must be selected for materials with high resistances to deformation or high melting temperatures (Vlcek et al. 2005).

1.6 Important Factors in CS

1.6.1 Deposition Efficiency

Deposition efficiency (DE) can be simply defined as the weight of particles successfully adhered to the substrate (m_s = final weight of the substrate – initial substrate weight) divided by the total weight of the initial feedstock particles (M_p). Mathematically, the deposition efficiency can be expressed as (Papyrin et al. 2006):

$$DE = \frac{m_s}{M_p} \times 100 \quad (1.1)$$

In order to improve adhesion, sand blasting is commonly used. However, this method has drawbacks, mainly from the contamination of the substrate by sand-blasted particles (Ghelichi and Guagliano 2009). Particle adhesion depends on many factors,

including the contact surface area, plastic deformation, yield stress, processing parameters (mainly the temperature and pressure of the gas), and the particle and substrate temperatures (Ghelichi and Guagliano 2009). In fact, the DE increases as the particle velocity significantly exceeds the critical velocity (Gilmore et al. 1999; Gärtner et al. 2006a; Fukanuma et al. 2006), as explained in the following.

1.6.2 Critical Velocity

The critical velocity V_{crit} is defined as the minimum particle velocity necessary for a material to adhere to the substrate (Papyrin et al. 2006). As demonstrated in Fig. 1.5, if the particle velocity is lower than V_{crit} , then either the particle makes impact and bounces back from the substrate or the particle hits the substrate and causes surface abrasion. However, if the particle velocity reaches or exceeds V_{crit} , then particle adhesion occurs. The value of V_{crit} depends on many factors, such as the material types of the substrate and feedstock powder, processing parameters, particle size, and substrate surface properties, like roughness (Gärtner et al. 2006a).

Assadi et al. (2003) used simulation modeling methods to predict V_{crit} . The critical velocity is associated with ASI, and the simulation results are summarized into the following equation:

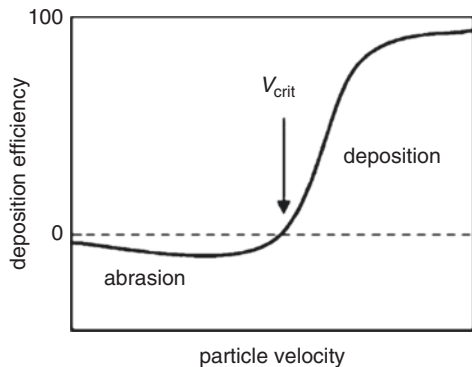
$$V_{crit} = 667 - 0.014\rho + 0.08(T_m - T_{Ref}) + 10^{-7}\sigma_{uts} - 0.4(T_i - T_{Ref}) \quad (1.2)$$

where ρ is the particle density, T_m is the melting temperature, T_{Ref} is the reference temperature at which the ultimate tensile strength is determined, σ_{uts} is the ultimate tensile strength, and T_i is the initial particle temperature.

Schmidt et al. (2006) developed another correlation for predicting V_{crit} :

$$V_{crit} = \sqrt{\left[4F_1\sigma_{uts} \left(1 - \frac{T_i - T_{Ref}}{T_m - T_{Ref}} \right) \rho_p^{-1} \right] + F_2c_p(T_m - T_i)} \quad (1.3)$$

Fig. 1.5 The effect of particle velocity on DE in CS (Gärtner et al. 2006a)



where σ_{uts} is the ultimate tensile strength, T_i is the initial particle temperature, T_{Ref} is the reference temperature at which the ultimate tensile strength is determined, T_m is the melting point of the particle, ρ_p is the density of the particle, c_p is the particle-specific heat capacity, and F_1 and F_2 are constants representing material-dependent calibration factors.

Figure 1.6 compares the calculated V_{crit} using Eqs. 1.2 and 1.3 with the experimental results of spray experiments and impact tests. The work by Assadi and his colleagues did not consider the size of particles as a significant factor in determining V_{crit} (Schmidt et al. 2006). In fact, smaller-size particles usually contain higher proportions of oxides, which hinder bonding (Blazynski 1983; Van Steenkiste and Smith 2004). Therefore, the prediction is much better using Eq. 1.3, especially when using tin and tantalum, which have significantly different properties than copper.

If the particle velocity greatly exceeds V_{crit} , this causes not only a higher DE, as illustrated in Fig. 1.5, but also a lower porosity (Kim et al. 2005b; Gärtner et al. 2006a). It is important to produce coatings with low porosities, as porosity influences the mechanical, electrical, and thermal properties of CS coatings (Li et al. 2006a; Sudharshan Phani et al. 2007). For example, a low-porosity coating generally exhibits higher hardness and better corrosion resistance compared to a more porous coating of the same material. The porosity level in CS coatings depends mainly on the feedstock material and processing parameters (Klinkov et al. 2005; Sudharshan Phani et al. 2007). However, it is possible to reduce the porosity of the as-sprayed coating using post-heat treatments (Li et al. 2006a; Novoselova et al. 2006; Sudharshan Phani et al. 2007; Sundararajan et al. 2009; Zahiri et al. 2009;

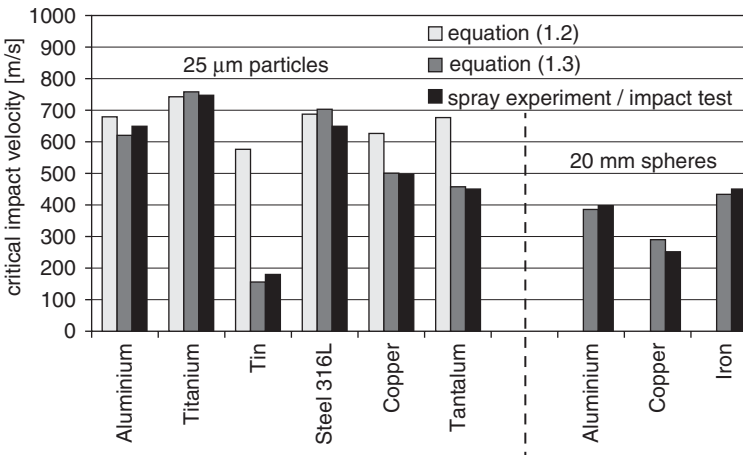


Fig. 1.6 Comparison of calculated critical velocity with experimental results of spray experiments and impact tests (Schmidt et al. 2006)

AL-Mangour et al. 2013; AL-Mangour et al. 2014). In addition, mechanical properties can be attained that approach bulk values for the coating material after post-CS heat treatment (Sudharshan Phani et al. 2007).

1.6.3 Gas Temperature and Pressure

Researchers have investigated the effects of different processing parameters on coating quality. Gas temperature and gas pressure have been studied the most extensively because they affect the particle impact velocity strongly (Gärtner et al. 2006a; Maev and Leshchynsky 2008; Wong et al. 2011; Meng et al. 2011). The typical gas used in CS is nitrogen, helium, or a mixture of the two (Borchers et al. 2008; Wong et al. 2011). Previous investigations have confirmed that higher particle impact velocities, generated by higher gas temperatures, produce coatings with higher DE and quality, as determined by lower porosity and higher strength (Stoltenhoff et al. 2002; Gärtner et al. 2006a, b; Borchers et al. 2008; Meng et al. 2011; Wong et al. 2011). High gas temperature is beneficial because it intensifies plastic deformation by promoting dislocation motion, recovery, and recrystallization (Gärtner et al. 2006b; Borchers et al. 2008; Meng et al. 2011).

For a given gas type and pressure, in order to obtain higher particle impact velocities, the gas temperature must be increased (Stoltenhoff et al. 2002; Meng et al. 2011). However, technical problems are associated with increased gas temperature, such as the sensitivity of the CS gun nozzle to high temperatures (i.e., material limitations), oxidation, and nitridation (Champagne 2007). On the other hand, it has been shown CS processing with helium gas produces a much higher particle impact velocity than that with nitrogen gas at the same temperature and pressure (Gilmore et al. 1999; Stoltenhoff et al. 2002; Li and Li 2003; Borchers et al. 2008; AL-Mangour et al. 2014), leading to a lower porosity. However, nitrogen is usually preferred because of the high cost of helium. Therefore, the challenge is to optimize the CS processing parameters to produce high-quality coatings using nitrogen gas.

The gas velocity v can be calculated using the equation below (Grujicic et al. 2004b):

$$v = \sqrt{\gamma RT / M_w} \quad (1.4)$$

where γ is the ratio of the constant-pressure- and the constant-volume-specific heats, which is approximately 1.66 for monoatomic gases (e.g., helium) and 1.4 for diatomic gases (e.g., nitrogen and oxygen). R is the gas constant (8314 J/kmol·K), T is the gas temperature, and M_w is the molecular weight of the gas. According to Eq. 1.4, increasing the temperature increases the velocity when all other parameters are constant. More interestingly, the critical velocity seems to decrease with increasing gas temperature, which may be because of thermal softening of the particles (Gärtner et al. 2006a; Lee et al. 2007). Most existing reports on the effect of gas temperature are based on numerical simulations (Sakaki and Shimizu 2001, Li et al. 2006b, Katanoda et al. 2007, Yin et al. 2010, Chuanshao et al. 2011,); therefore, further experimental analysis should be performed to establish better understanding.

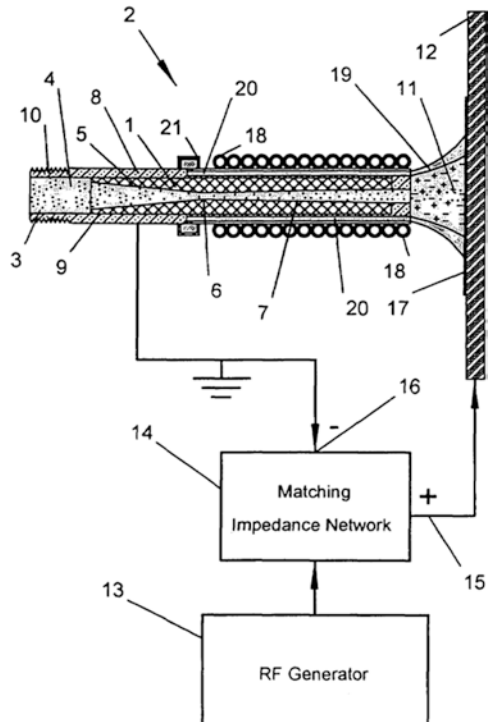
1.7 Enhancements to the CS Process

With the development of the CS process, numerous studies have been undertaken for process enhancement. Current enhanced CS processes include kinetic metallization (KM), pulsed gas dynamic spraying (PGDS), and vacuum CS (VCS) (Moridi et al. 2014).

KM (Fig. 1.7) differs from other forms of CS in that it uses a convergent barrel nozzle under choked flow conditions to achieve a velocity of Mach 1 (Moridi et al. 2014). To compensate for friction, the nozzle is also slightly diverged from a straight path. To accelerate gas velocity, other CS processes use de Laval nozzles. Coatings made with KM have demonstrated stronger particle–particle and particle–substrate bonds (Wang et al. 2010).

Multiple patents exist for KM processes globally. One example, by Inovati (2016), uses a special design comprising a set of friction-aided spouts for depositing the particles, where metallic particles carried in low-pressure helium or nitrogen gas (70–130 psi) within the nozzle can reach a maximum speed of 1000 m/s. The amount of inert carrier gas used in the acceleration of particles by KM is greatly reduced compared to those in supersonic methods for the same purposes (Irissou et al. 2008). The major deviation of KM from other CS processes is the lower kinetic energy of particle impact involved. This is achieved by slightly increasing the temperature of the powder particles used, allowing easy plastic deformation.

Fig. 1.7 KM schematic (Tapphorn and Gabel 2007)



PGDS (Fig. 1.8) warms the feedstock particles to a transitional temperature higher than the temperatures encountered in conventional CS processes (Jodoin et al. 2007). Moreover, it promotes elevation in plastic deformation while maintaining the impact speed. The process also utilizes non-motionless pressure effects to produce concurrently higher pressure at the exit point, as opposed to conventional CS processes, which use perpetual fixed-flow exits (Yin et al. 2016). Unlike the case of CS, it is possible to accomplish elevated particle impact temperatures with PGDS owing to the gas compression that causes the propelling flow. Thus, it is expected that PGDS could permit particles to reach elevated impact speeds and intermediate impact temperatures, which could lead to relatively lower critical speeds than those in CS, thus improving the plastic deformation upon impact with the underlying substrate at a constant impact velocity.

VCS (Fig. 1.9) takes place in a vacuum cistern. The substrate is placed opposite to a spurt with a spray gun at one end within the vacuum chamber; the spray gun deposits the metal particles. Here, the metallic powdered particles in the vacuum chamber are accelerated to a high velocity so that, at the point of impact with the substrate, they undergo deformation on the active surface of the substrate and create strong bonds. VCS technology is preferred for the coating of thin films. The vacuum tank allows for recovery of gases and collection of oversprays (Muehlberger 2004). VCS differs from other CS systems in allowing for the deposition of nanoscale particles. The most recent form of VCS is referred to as the aerosol deposition method (Akedo et al. 2008). Detailed information on the patent can be found elsewhere (Muehlberger 2004).

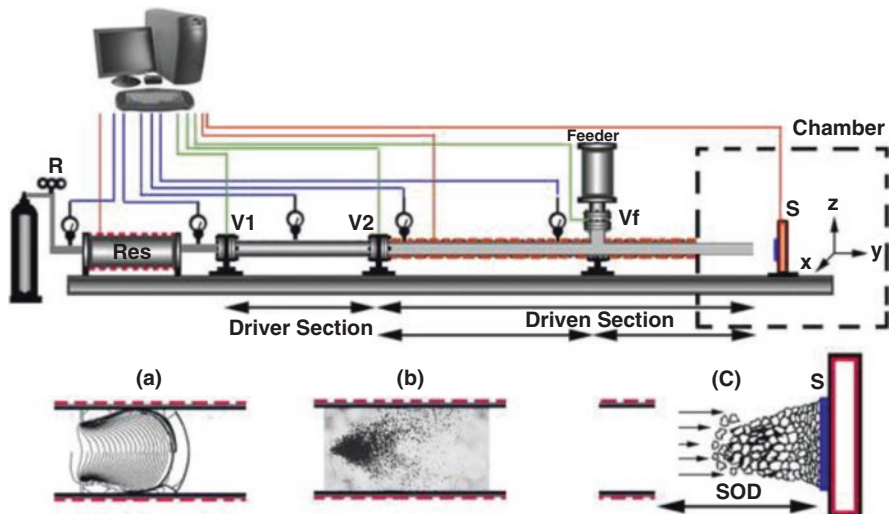


Fig. 1.8 Schematic of the PGDS technique (a–c) represents shockwave generation, particles flowing under compressed gas, and coating buildup, respectively, which occur during one pulse (Jodoin et al. 2007)

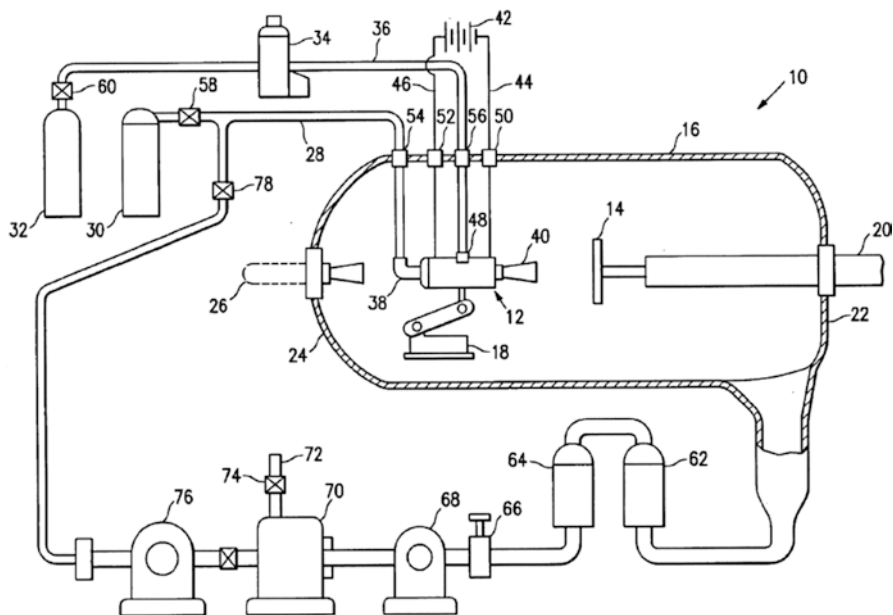


Fig. 1.9 VCS setup (Muehlberger 2004)

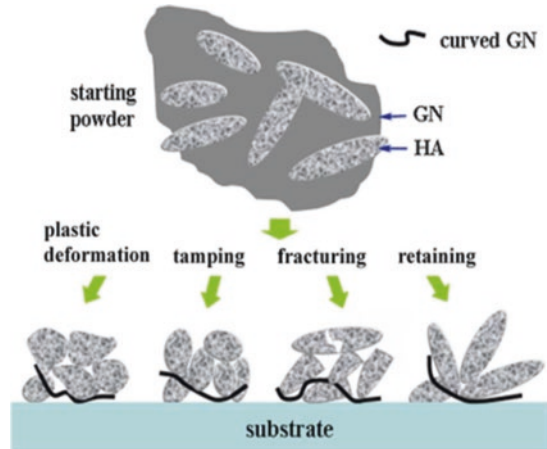
A recent application of VCS was in hydroxyapatite (HA) coatings utilized in the biomedical sector (Choudhuri et al. 2009). The VCS-deposited HA nanosheets showed significant deformation. The structures were thick with investigations revealing the formation of dense deposits of nanosheets. The study showed that the application of graphene nanosheets (GN) significantly improved the fracture strength and exhibited better HA coatings that covered fractures with deposits. VCS to achieve a composite with GN and HA (Fig. 1.10) with thin film coatings was suggested for use in regenerating tough tissues (Liu et al. 2014).

1.8 Recent Developments in Cold Spray Technology

1.8.1 Shockwave-Induced Spraying

The development of shockwave-induced spraying (SISP) is among the latest advancements in material deposition. The method enables the solid-state deposition of materials beyond typical CS, with elevated deposition rates and efficiencies. It is anticipated that SISP will become a favored solid-state spraying process for applications requiring high productivity at low cost. Other possible advances include the development of smaller, more portable, low-pressure CS units for field use and other applications.

Fig. 1.10 Schematic demonstrating the formation mechanisms of the HA–GN nanocomposite coating (Liu et al. 2014)



SISP involves the production of streams of shockwaves using a regulator that rapidly opens and closes to allow a flow of inert gas under high pressure. The generated stream of shockwaves passes through a straight outlet, compressing the gas already in the nozzle. This creates an intensely heated pulse at supersonic speed, with a frequency of $\sim 10\text{--}30$ Hz. This pulse travels through the powder particles, heating them below their thermal deformation point and accelerating them as they are carried toward the outlet. Conventional CS processing, meanwhile, requires diverging–converging outlets (which lead to a higher exit pressure), which SISP does not (Karimi et al. 2011).

SISP works such that the less supersonic system dictates the rate of the gas flow as well as the number of generated pulse streams; however, heating of the powdered particles is due to the compression produced by the shockwaves. The SISP system allows the gas in the nozzle to cool as it expands toward the diverging de Laval outlet. The critical velocity of the powdered particles is reduced, allowing bonding of the solid caused by movement of heated particles through the nozzle. SISP utilizes both kinetic and thermal energy from the solid particles, promoting excellent deposition of solid-state particles on numerous materials. The greatest benefit of this system is its minimization of energy consumption, thus reducing operation costs in terms of energy, as compared to CS (Karimi et al. 2011).

1.8.2 Nozzle Design

Improvements in the nozzle design have promoted relatively higher deposition velocities as well as the capability to deposit bigger particles (Lupoi and O’Neill 2011). This has greatly improved the operating ability by elevating the spray location, although it limits the prevailing angle of the nozzle divergence to sustain a stable gas flow. Nozzle modifications are made by attaching pneumatic channels to the individual gas and powdered mixture feed channels and the corresponding

common pre-chamber. Fluid dynamic models were employed to design nozzles with substantially elevated particle velocities, creating denser coatings and higher deposition efficiency. Augmentation of the length of the nozzle has been demonstrated to significantly affect the particle velocity. For instance, by increasing the length of the central nozzle from 82 mm to 211 mm with nitrogen as the carrier gas, the computed velocity of a 12 μm copper particle is increased from 553 m/s to 742 m/s (Schleef et al. 2014): a 33% increase. The materials also limit the practical length of existing nozzles (Klinkov et al. 2005). Supplementary nozzle advancements entail the utilization of modern nozzle designs, such as convergent barrels, to enhance powder flow via the nozzle and design optimization to minimize gas flow friction via the nozzle (Li et al. 2006b). An increase in the gas temperature typically causes a proportional increase in the gas velocity; nozzle design can be improved by including gas heating (Lupoi 2014).

An experimental setup used to estimate the efficient nozzle design geometry values for a CS process is depicted in Fig. 1.11. A_i and A_e denote the cross-sectional areas of the inlet and outlet, respectively; L_c and L_d are the lengths of the converging and diverging nozzle sections, respectively; A^* represents the cross-sectional area of the nozzle throat (Meyer and Lupoi 2015) (Table 1.2).

The depositional efficiency tests from the three experiments show that the CS process attains maximum depositional efficiency with nozzle dimensions corresponding to those of N3, as shown in Table 1.3.

Thus, the nozzle designed mainly improved the coating process. The relatively elevated particle speed from the advanced plunger design promoted a greater covering density, thereby improving the mechanical properties (Champagne and Helfrich 2016). CS nozzle design also helps increase operation capability by maintaining the stability of gas flow.

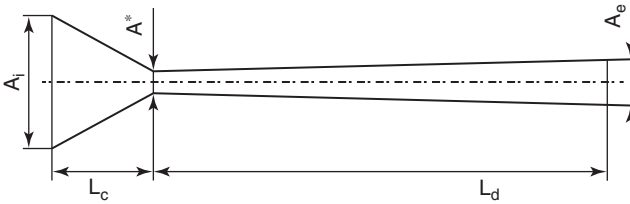


Fig. 1.11 CS nozzle geometry (Meyer and Lupoi 2015)

Table 1.2 Geometrical details of the nozzles *N1*, *N2*, and *N3*

Nozzle	A_i [mm ²]	L_c [mm]	A^* [mm ²]	L_d [mm]	A_e [mm ²]
<i>N1</i>	314	30	3.1	180	28.3
<i>N2</i>	44.2	15.5	5.7	190	47.8
<i>N3</i>	314	20	5.7	190	47.8

Meyer and Lupoi (2015)

Table 1.3 Depositional efficiency comparison

Nozzle	DE [%]
N1	16.3
N2	32.5
N3	33.5

Lupoi (2014)

1.9 CS Process Advancements and Applications

CS processes have led to the emergence of sprayed composite materials. CS allows the fabrication of tungsten/copper composites among the best materials for the production of heat sinks owing to their high heat conductivities and very low coefficients of thermal expansion. Previously, infiltration methods were used to produce such composites; this was costly because of the high temperatures used and the products suffered from low deposition and densification. CS processes are less expensive in producing composites with end qualities superior to those of composites created by the infiltration method (Kang and Kang 2003).

Another recent promising work is the metallization of low-weight and high-strength carbon fiber composites, which are promising for the aerospace industry. Traditional manufacturing processes are difficult to apply in forming coatings of fiber composite materials because they are time-consuming, labor-intensive, and expensive; however, the metallization of carbon fiber-reinforced polymer (CFRP) composites helps increase the conductivity of the fuselage in aerospace engineering. CS processes have helped to solve problems of oxidation and weight increases in CFRP structures. Through the CS process, sprayed conductive metal particles remain in the solid state, forming a thin layer of non-oxidized conductive metal (Archambault et al. 2016) (Fig. 1.12).

In the biomedical field, AL-Mangour et al. (2013) proposed the use of Co–Cr and stainless steel alloy mixtures for medical implants. Co–Cr is more resistant to corrosion than stainless steel but is also more difficult to manufacture and more expensive. CS allows cheap and easy improvement of stainless steel in terms of corrosion resistance and strength by combining it with Co–Cr. This could ultimately lead to new biomaterials in the future.

CS is also used to increase the resistance to dry sliding wear of Ni–WC composite materials. According to experimental results, the inclusion of WC particles through CS stabilized the coefficient of friction and decreased the rate of wear. These effects are attributed to the creation of a cohesive and stable mechanically mixed layer on the top of the Ni–WC coating wear track (Alidokht et al. 2016).

Magnesium alloys also have high strength-to-weight ratios, making them suitable candidates for use in the transport industry. However, they are highly susceptible to wear and corrosion. CS processing could allow the use of such alloys because it produces composites with stronger bonds and greater resistance to wear and corrosion. According to Wang et al. (2010), the addition of Al₂O₃ to coatings has been shown to increase the strength of Mg–Al bonds, thereby strengthening the fabricated alloys.

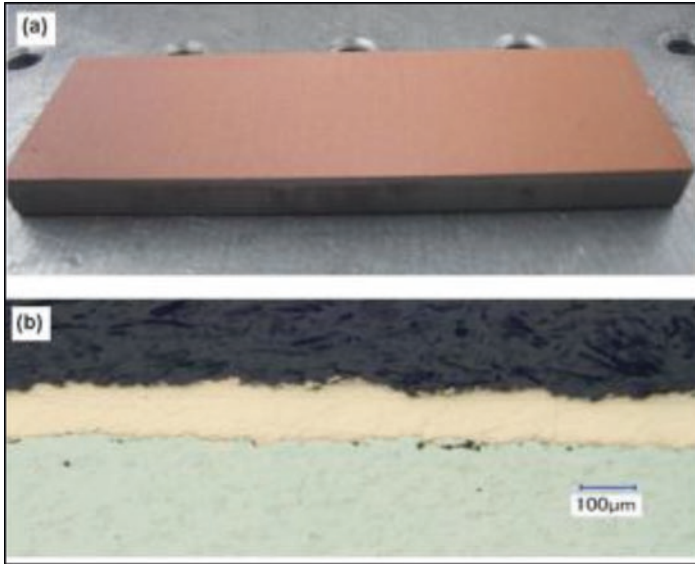


Fig. 1.12 Typical copper coating on Invar substrate obtained by CS process: (a) plane view and (b) cross-sectional image, revealing the quality of the deposited metallic layer (Archambault et al. 2016)

CS can also be applied to additive manufacturing, which assembles an object as a whole rather than through the creation of component parts that are joined together. Research has shown that CS can create three-dimensional shapes of varying geometries. Robotic control can help to direct the nozzle to follow the contours of the desired shape. Several layers of metal are continuously deposited to achieve the desired thickness. Machining is performed on the resulting object to achieve the desired finish (Champagne et al. 2010). Recent research (Champagne and Helfrich 2016) suggested that additive manufacturing would be the most commercially viable option for the application of CS processes, if further advancements occur to refine CS deposits.

With the evolution of technology, it is expected that the applicability of CS will expand to more advanced fields such as those involving wind energy, photovoltaic energy, architecture, and medicine. For instance, in photovoltaic applications, the technology can be applied for the fabrication of intricate conductive designs in solar cells. Wind power production might be able to utilize CS to improve surface performance in elements manufactured from complex polymer–matrix composites. The future of CS depends on its potential to deposit advanced materials onto a wide range of substrates with the least thermal cost and penalty. These factors will define the opportunities and future directions of CS.

References

- Akedo J, Nakano S, Jaehyuk P, Ashida K (2008) The aerosol deposition method. *Synthes Engl Ed* 1:121–130. <https://doi.org/10.5571/syntheng.1.121>

- Alidokht SA, Manimunda P, Vo P, Yue S, Chromik RR (2016) Cold spray deposition of a Ni-WC composite coating and its dry sliding wear behavior. *Surf Coat Technol* 308:424–434. <https://doi.org/10.1016/j.surfcoat.2016.09.089>
- Alkhimov A, Kosarev V, Papyrin A (1990) A method of cold gas-dynamic spraying. *Dokl Akad Nauk SSSR* 315:1062–1065
- AL-Mangour B, Mongrain R, Irissou E, Yue S (2013) Improving the strength and corrosion resistance of 316L stainless steel for biomedical applications using cold spray. *Surf Coat Technol* 216:297–307. <https://doi.org/10.1016/j.surfcoat.2012.11.061>
- AL-Mangour B, Vo P, Mongrain R, Irissou E, Yue S (2014) Effect of heat treatment on the microstructure and mechanical properties of stainless steel 316L coatings produced by cold spray for biomedical applications. *J Therm Spray Technol* 23:641–652. <https://doi.org/10.1007/s11666-013-0053-2>
- Amodeo RJ, Ghoniem NM (1990) Dislocation dynamics. I. A proposed methodology for deformation micromechanics. *Phys Rev B* 41:6958–6967. <https://doi.org/10.1103/PhysRevB.41.6958>
- Archambault G, Jodoin B, Gaydos S, Yandouzi M (2016) Metallization of carbon fiber reinforced polymer composite by cold spray and lay-up molding processes. *Surf Coat Technol* 300:78–86. <https://doi.org/10.1016/j.surfcoat.2016.05.008>
- Assadi H, Gärtner F, Stoltenhoff T, Kreye H (2003) Bonding mechanism in cold gas spraying. *Acta Mater* 51:4379–4394. [https://doi.org/10.1016/S1359-6454\(03\)00274-X](https://doi.org/10.1016/S1359-6454(03)00274-X)
- Bae G, Xiong Y, Kumar S, Kang K, Lee C (2008) General aspects of interface bonding in kinetic sprayed coatings. *Acta Mater* 56:4858–4868. <https://doi.org/10.1016/j.actamat.2008.06.003>
- Bae G, Kumar S, Yoon S, Kang K, Na H, Kim H-J, Lee C (2009) Bonding features and associated mechanisms in kinetic sprayed titanium coatings. *Acta Mater* 57:5654–5666. <https://doi.org/10.1016/j.actamat.2009.07.061>
- Blazynski T (1983) Explosive welding, forming and compaction. Applied Science Publishers, London
- Borchers C, Gärtner F, Stoltenhoff T, Kreye H (2004) Microstructural bonding features of cold sprayed face centered cubic metals. *J Appl Phys* 96:4288. <https://doi.org/10.1063/1.1789278>
- Borchers C, Gärtner F, Stoltenhoff T, Kreye H (2005) Formation of persistent dislocation loops by ultra-high strain-rate deformation during cold spraying. *Acta Mater* 53:2991–3000. <https://doi.org/10.1016/j.actamat.2005.02.048>
- Borchers C, Schmidt T, Gärtner F, Kreye H (2008) High strain rate deformation microstructures of stainless steel 316L by cold spraying and explosive powder compaction. *Appl Phys A: Mater Sci Proc* 90:517–526. <https://doi.org/10.1007/s00339-007-4314-0>
- Champagne VK (2007) The cold spray materials deposition process: fundamentals and applications. CRC Press, Cambridge, England
- Champagne V, Helfritsch D (2016) The unique abilities of cold spray deposition. *Int Mater Rev* 61:437–455. <https://doi.org/10.1080/09506608.2016.1194948>
- Champagne V, Helfritsch D, Wienhold E, Dehaven J (2010) The development of nickel-aluminum reactive material by cold spray process. Army Research Laboratory Technical Report ARL-TR-5189
- Choudhuri A, Mohanty P, Karthikeyan J (2009) Bio-ceramic composite coatings by cold spray technology. *Proc Int Thermal Spray Conf, Japan Association for Earthquake Engineering*
- Chuanshao L, Song C, Jianxin Z (2011) Numerical simulation of gas-particle two phase flow in aluminum-oxide ceramics powder spraying process. *Consumer Electron Comm Netw (CECNet)*, 2011 Int Conf 16–18 April 2011. 4216–4218. doi:<https://doi.org/10.1109/CECNET.2011.5768755>
- Dykhuizen RC, Smith MF (1998) Gas dynamic principles of cold spray. *J Therm Spray Technol* 7:205–212. <https://doi.org/10.1361/105996398770350945>
- Fukanuma H, Ohno N, Sun B, Huang R (2006) In-flight particle velocity measurements with DPV-2000 in cold spray. *Surf Coat Technol* 201:1935–1941. <https://doi.org/10.1016/j.surfcoat.2006.04.035>
- Gärtner F, Stoltenhoff T, Schmidt T, Kreye H (2006a) The cold spray process and its potential for industrial applications. *J Therm Spray Technol* 15:223–232. <https://doi.org/10.1361/105996306X108110>
- Gärtner F, Stoltenhoff T, Voyer J, Kreye H, Riekehr S, Koçak M (2006b) Mechanical properties of cold-sprayed and thermally sprayed copper coatings. *Surf Coat Technol* 200:6770–6782. <https://doi.org/10.1016/j.surfcoat.2005.10.007>
- Ghelichi R, Guagliano M (2009) Coating by the cold spray process: a state of the art. *Fratt Integr Strutt* 8:30–44. <https://doi.org/10.3221/IGF-ESIS.08.03>

- Gilmore DL, Dykhuizen RC, Neiser RA, Smith MF, Roemer TJ (1999) Particle velocity and deposition efficiency in the cold spray process. *J Therm Spray Technol* 8:576–582. <https://doi.org/10.1361/105996399770350278>
- Grujicic M, Saylor JR, Beasley DE, DeRosset WS, Helfritsch D (2003) Computational analysis of the interfacial bonding between feed-powder particles and the substrate in the cold-gas dynamic-spray process. *Appl Surf Sci* 219:211–227. [https://doi.org/10.1016/S0169-4332\(03\)00643-3](https://doi.org/10.1016/S0169-4332(03)00643-3)
- Grujicic M, Zhao CL, DeRosset WS, Helfritsch D (2004a) Adiabatic shear instability based mechanism for particles/substrate bonding in the cold-gas dynamic-spray process. *Mater Des* 25:681–688. <https://doi.org/10.1016/j.matdes.2004.03.008>
- Grujicic M, Zhao CL, Tong C, DeRosset WS, Helfritsch D (2004b) Analysis of the impact velocity of powder particles in the cold-gas dynamic-spray process. *Mater Sci Eng A* 368:222–230. <https://doi.org/10.1016/j.msea.2003.10.312>
- Hussain T, McCartney DG, Shipway PH, Zhang D (2009) Bonding mechanisms in cold spraying: the contributions of metallurgical and mechanical components. *J Therm Spray Technol* 18:364–379. <https://doi.org/10.1007/s11666-009-9298-1>
- Inovati (2016) Kinetic metallization: coatings once thought impossible. Inovati Innovative Technology Inc. <http://www.inovati.com>. Accessed 8 Apr 2017
- Irissou E, Legoux J-G, Arsenault B, Moreau C (2007) Investigation of al-Al₂O₃ cold spray coating formation and properties. *J Therm Spray Technol* 16:661–668. <https://doi.org/10.1007/s11666-007-9086-8>
- Irissou E, Legoux J-G, Ryabinin AN, Jodoin B, Moreau C (2008) Review on cold spray process and technology: part I—intellectual property. *J Therm Spray Technol* 17:495–516. <https://doi.org/10.1007/s11666-008-9203-3>
- Jodoin B, Richer P, Bérubé G, Ajdelsztajn L, Erdi-Betchi A, Yandouzi M (2007) Pulsed-gas dynamic spraying: process analysis, development and selected coating examples. *Surf Coat Technol* 201:7544–7551. <https://doi.org/10.1016/j.surfcoat.2007.02.033>
- Kang H-K, Kang SB (2003) Tungsten/copper composite deposits produced by a cold spray. *Scr Mater* 49:1169–1174. <https://doi.org/10.1016/j.scriptamat.2003.08.023>
- Karimi M, Jodoin B, Rankin G (2011) Shock-wave-induced spraying: modeling and physics of a new spray process. *J Therm Spray Technol* 20:866–881. <https://doi.org/10.1007/s11666-011-9622-4>
- Katanoda H, Fukuhara M, Iino N (2007) Numerical study of combination parameters for particle impact velocity and temperature in cold spray. *J Therm Spray Technol* 16:627–633. <https://doi.org/10.1007/s11666-007-9087-7>
- Kim H-J, Lee C-H, Hwang S-Y (2005a) Fabrication of WC-co coatings by cold spray deposition. *Surf Coat Technol* 191:335–340. <https://doi.org/10.1016/j.surfcoat.2004.04.058>
- Kim H-J, Lee C-H, Hwang S-Y (2005b) Superhard nano WC–12%co coating by cold spray deposition. *Mater Sci Eng A* 391:243–248. <https://doi.org/10.1016/j.msea.2004.08.082>
- Klinkov SV, Kosarev VF, Rein M (2005) Cold spray deposition: significance of particle impact phenomena. *Aerosp Sci Technol* 9:582–591. <https://doi.org/10.1016/j.ast.2005.03.005>
- Lee J, Shin S, Kim H, Lee C (2007) Effect of gas temperature on critical velocity and deposition characteristics in kinetic spraying. *Appl Surf Sci* 253:3512–3520. <https://doi.org/10.1016/j.apsusc.2006.07.061>
- Li C-J, Li W-Y (2003) Deposition characteristics of titanium coating in cold spraying. *Surf Coat Technol* 167:278–283. [https://doi.org/10.1016/S0257-8972\(02\)00919-2](https://doi.org/10.1016/S0257-8972(02)00919-2)
- Li W-Y, Li C-J, Liao H (2006a) Effect of annealing treatment on the microstructure and properties of cold-sprayed Cu coating. *J Therm Spray Technol* 15:206–211. <https://doi.org/10.1361/105996306X108066>
- Li W-Y, Liao H, Wang H-T, Li C-J, Zhang G, Coddet C (2006b) Optimal design of a convergent-barrel cold spray nozzle by numerical method. *Appl Surf Sci* 253:708–713. <https://doi.org/10.1016/j.apsusc.2005.12.157>
- Liu Y, Huang J, Li H (2014) Nanostructural characteristics of vacuum cold-sprayed hydroxyapatite/graphene-nanosheet coatings for biomedical applications. *J Therm Spray Technol* 23:1149–1156. <https://doi.org/10.1007/s11666-014-0069-2>

- Lupoi R (2014) Current design and performance of cold spray nozzles: experimental and numerical observations on deposition efficiency and particle velocity. *Surf Eng* 30:316–322. <https://doi.org/10.1179/1743294413Y.0000000214>
- Lupoi R, O'Neill W (2011) Powder stream characteristics in cold spray nozzles. *Surf Coat Technol* 206:1069–1076. <https://doi.org/10.1016/j.surfcoat.2011.07.061>
- Maev RG, Leshchynsky V (2008) Introduction to low pressure gas dynamic spray: physics & technology. Weinheim (Germany), Wiley-VCH 234
- Marx S, Paul A, Köhler A, Hüttl G (2006) Cold spraying: innovative layers for new applications. *J Therm Spray Technol* 15:177–183. <https://doi.org/10.1361/105996306X107977>
- Meng X, Zhang J, Zhao J, Liang Y, Zhang Y (2011) Influence of gas temperature on microstructure and properties of cold spray 304SS coating. *J Mater Sci Technol* 27:809–815. [https://doi.org/10.1016/S1005-0302\(11\)60147-3](https://doi.org/10.1016/S1005-0302(11)60147-3)
- Meyer M, Lupoi R (2015) An analysis of the particulate flow in cold spray nozzles. *Mech Sci* 6:127–136. <https://doi.org/10.5194/ms-6-127-2015>
- Moridi A, Hassani-Gangaraj SM, Guagliano M, Dao M (2014) Cold spray coating: review of material systems and future perspectives. *Surf Eng* 30:369–395. <https://doi.org/10.1179/1743294414Y.0000000270>
- Muehlberger E (2004) Method and apparatus for low pressure cold spraying. US Patent 6759085 B2, 6 Jul 2004
- Novoselova T, Fox P, Morgan R, O'Neill W (2006) Experimental study of titanium/aluminium deposits produced by cold gas dynamic spray. *Surf Coat Technol* 200:2775–2783. <https://doi.org/10.1016/j.surfcoat.2004.10.133>
- Papyrin A, Kosarev V, Klinkov S, Alkhimov A, Fomin V (2006) Cold spray technology. Elsevier. Amsterdam, The Netherlands
- Sakaki K, Shimizu Y (2001) Effect of the increase in the entrance convergent section length of the gun nozzle on the high-velocity oxygen fuel and cold spray process. *J Therm Spray Technol* 10:487–496. <https://doi.org/10.1361/105996301770349268>
- Sampath S, Jiang XY, Matejcek J, Prchlik L, Kulkarni A, Vaidya A (2004) Role of thermal spray processing method on the microstructure, residual stress and properties of coatings: an integrated study for Ni–5 wt.%Al bond coats. *Mater Sci Eng A* 364:216–231. <https://doi.org/10.1016/j.msea.2003.08.023>
- Schleef S, Jaggi M, Löwe H, Schneebeli M (2014) An improved machine to produce nature-identical snow in the laboratory. *J Glaciol* 60:94–102. <https://doi.org/10.3189/2014JoG13J118>
- Schmidt T, Gärtner F, Assadi H, Kreye H (2006) Development of a generalized parameter window for cold spray deposition. *Acta Mater* 54:729–742. <https://doi.org/10.1016/j.actamat.2005.10.005>
- Stoltenhoff T, Kreye H, Richter HJ (2002) An analysis of the cold spray process and its coatings. *J Therm Spray Technol* 11:542–550. <https://doi.org/10.1361/105996302770348682>
- Sudharshan Phani P, Srinivasa Rao D, Joshi SV, Sundararajan G (2007) Effect of process parameters and heat treatments on properties of cold sprayed copper coatings. *J Therm Spray Technol* 16:425–434. <https://doi.org/10.1007/s11666-007-9048-1>
- Sundararajan G, Sudharshan Phani P, Jyothirmayi A, Gundakaram RC (2009) The influence of heat treatment on the microstructural, mechanical and corrosion behaviour of cold sprayed SS 316L coatings. *J Mater Sci* 44:2320–2326. <https://doi.org/10.1007/s10853-008-3200-2>
- Taphorn RM, Gabel H (2007) System and process for solid-state deposition and consolidation of high velocity powder particles using thermal plastic deformation. US Patent 6915964 B2, 12 Jul 2005
- Van Steenkiste T, Smith J (2004) Evaluation of coatings produced via kinetic and cold spray processes. *J Therm Spray Technol* 13:274–282. <https://doi.org/10.1361/10599630419427>
- Van Steenkiste TH, Smith JR, Teets RE (2002) Aluminum coatings via kinetic spray with relatively large powder particles. *Surf Coat Technol* 154:237–252. [https://doi.org/10.1016/S0257-8972\(02\)00018-X](https://doi.org/10.1016/S0257-8972(02)00018-X)
- Vlcek J, Gimeno L, Huber H, Lugscheider E (2005) A systematic approach to material eligibility for the cold-spray process. *J Therm Spray Technol* 14:125–133. <https://doi.org/10.1361/10599630522738>

- Wang Q, Spencer K, Birbilis N, Zhang M-X (2010) The influence of ceramic particles on bond strength of cold spray composite coatings on AZ91 alloy substrate. *Surf Coat Technol* 205:50–56. <https://doi.org/10.1016/j.surfcoat.2010.06.008>
- Wong W, Irissou E, Ryabinin AN, Legoux J-G, Yue S (2011) Influence of helium and nitrogen gases on the properties of cold gas dynamic sprayed pure titanium coatings. *J Therm Spray Technol* 20:213–226. <https://doi.org/10.1007/s11666-010-9568-y>
- Yandouzi M, Sansoucy E, Ajdelsztajn L, Jodoin B (2007) WC-based cermet coatings produced by cold gas dynamic and pulsed gas dynamic spraying processes. *Surf Coat Technol* 202:382–390. <https://doi.org/10.1016/j.surfcoat.2007.05.095>
- Yin S, Wang X-F, Li W-Y, Xu B-P (2010) Numerical study on the effect of substrate angle on particle impact velocity and normal velocity component in cold gas dynamic spraying based on CFD. *J Therm Spray Technol* 19:1155–1162. <https://doi.org/10.1007/s11666-010-9510-3>
- Yin S, Meyer M, Li W, Liao H, Lupoi R (2016) Gas flow, particle acceleration, and heat transfer in cold spray: a review. *J Therm Spray Technol* 25:874–896. <https://doi.org/10.1007/s11666-016-0406-8>
- Zahiri SH, Antonio CI, Jahedi M (2009) Elimination of porosity in directly fabricated titanium via cold gas dynamic spraying. *J Mater Process Technol* 209:922–929. <https://doi.org/10.1016/j.jmatprotec.2008.03.005>
- Zou Y, Qin Q, Irissou E, Legoux J-G, Yue S, Szpunar JA (2009) Dynamic recrystallization in the particle/particle interfacial region of cold-sprayed nickel coating: electron backscatter diffraction characterization. *Scr Mater* 61:899–902. <https://doi.org/10.1016/j.scriptamat.2009.07.020>